Characteristic crystal orientation of folia in oyster shell, *Crassostrea gigas*

Seung Woo Lee [a], Gyeung Ho Kim [b], Cheong Song Choi [a],*

[a] *Department of Chemical and Biomolecular Engineering, Sogang University, Seoul, Korea*
[b] *Nano-Materials Reserch Center, Korea Institute of Science and Technology, Seoul, Korea*

Abstract

The thin sheets of calcite, termed folia, that make up much of the shell of an oyster are composed of foliated lath. Folia of the giant Pacific oyster (*Crassostrea gigas*) were examined using TEM (transmission electron microscopy) and tested using microindentation and nanoindentation techniques. Analysis of the Kikuchi patterns obtained from the folia showed that there are two types (type I and type II) of preferred orientation, with an angle of around 70° between them. Nanoindentation tests showed that the folia exhibit a hardness of about 3 GPa and elastic modulus of about 73 GPa. Microcracks were generated using a microindenter in order to study the fracture mechanisms of the folia. Following on from these investigations, fracture mechanisms are discussed in conjunction with the correlation between preferred orientation and structural characteristics during cracking of the folia. Comparing the morphology and the polymorphism with nacre (also known as mother of pearl), the advantages of the relatively fast crystal growth and less amount of organic matrix in folia may have interesting implications for the development of sophisticated synthetic materials.
© 2007 Elsevier B.V. All rights reserved.

Keywords: Folia; Orientation; Kikuchi pattern; Calcite; Mechanical properties; Oyster shell

1. Introduction

The natural world has long been a source of ideas and inspiration for engineering design. The popularity of designs that mimic living systems is due to the fact that these designs have been refined and perfected over the course of millions of years of evolutionary selection [1–5].

One objective of shell research is to understand how shells are formed. A variety of studies have shown that biological composites such as shell have particularly favorable mechanical properties. However, current engineering methodologies for the synthesis of such complicated, hierarchical structures are not very practical, since the microarchitecture and toughening mechanisms of seashells have not been well explored or understood. This limits the scope for further development and improvement of nanocomposite designs. The microstructure and fracture mechanism of the oyster shell have attracted considerable attention due to their similar laminated appearance, but with the difference that they are composed of biogenic calcite, rather than aragonite, crystals. However, calcite could be more beneficial than aragonite because calcite is secreted more economically (i.e., calcite fills a larger volume per mole than aragonite does) [6] and exhibits a growth rate, at equal thermodynamic driving force, that is more than three times faster than that of aragonite [7]. Therefore, extensive studies on the laminated layer of oyster shell are needed in order to understand the microstructure and corresponding mechanical behavior of seashells. Oyster shell is mainly composed of calcite, as opposed to the aragonite in nacre. In addition, the amount of organic phase is much smaller in oyster shell than in nacre [8]. Thus, the mechanism of energy absorption of folia and nacre during crack propagation is different. Characterization of the oyster shell may provide valuable information which could be readily applicable to the design of ceramic composite materials in which the high content of ceramic constituents makes these materials inherently brittle. Careful control of microstructure is essential to improve the crack resistance of ceramic composite materials and the laminated structure in oyster shell could be an excellent example.

The primary objective of this study was to perform a crystallographic and mechanical investigation of the folia of oyster shell in order to gain some insight into the novel design concept of microstructures with high crack resistance, which could ultimately provide the information needed to improve the mechanical properties of advanced ceramic matrix composites. In this study, the folia forming a boundary layer against the adduct muscle scar were analyzed in detail.

2. Materials and methods

All tests were performed on folia under myostracum of adductor muscle scar, *Crassostrea gigas*, cultivated in Namhae, in the southern coastal region of Korea. To separate chalky layer, specimens were finely ground and separated using an electric mill, cutting knife. To identify mineralogy of separated specimens, optical microscope (VL-11S) was used. Specimens, 5.0 mm wide, 20.0 mm long and 0.7 mm thick in size were washed with distilled water and air dried at room temperature.

2.1. TEM (transmission electron microscope)

To prepare TEM samples, 2–3 mm wide pieces were cut first with a precision diamond saw. Small pieces were collected and inserted into the titanium grid (3 mm grid) with cut surface facing upward. Sample was secured with thermosetting epoxy (EpoxyBond 110, Allied HighTech Products, CA, USA) at 120 C for 10 minutes into the titanium grid for further polishing. Grid with sample mounted in the center was ground to below 100 μm, and then dimpled to below 60 μm in thickness. The dimpling procedure could produce a thin central region in the grid while leaving a thick supporting rim to protect the sample from damage. After dimpling, the samples were ion beam polished to generate a large electron transparent region using low angle ion beam milling. The double-sided milling (Technorg Linda, IV-3, Hungary) was used with incident beam angle of 5°. The voltage of ion beam was kept at 10 kV and total beam current of 2 mA. Specimen rocking was employed to minimize the differential thinning effect parallel to the laminated structure. After perforation of TEM sample, thin carbon coating was applied to the specimen to prevent electrical charging during observation in the TEM.

2.2. Data acquisition and analysis

The prepared sample was mounted into the double tilting holder. The sample was observed in a Tecnai F20 G2 FEG-TEM (FEI company, The Nertherlands) operating at 200 kV for BF imaging and high resolution imaging and 120 kV for Kikuchi pattern observations. Image recording was done by CCD (Gatan USC 1000, Gatan Inc., CA, USA). Si as a standard sample was used for calibration of camera length. Kikuchi pattern matching program (TOCA, TSL Inc., UT, USA) was used. Kikuchi pattern simulation programs (Electron Diffraction by J. P. Morniroli, UMR, CNRS, Lille, France, and JEMS by P. Stadelmann, CIME-EPFL,CH-1015
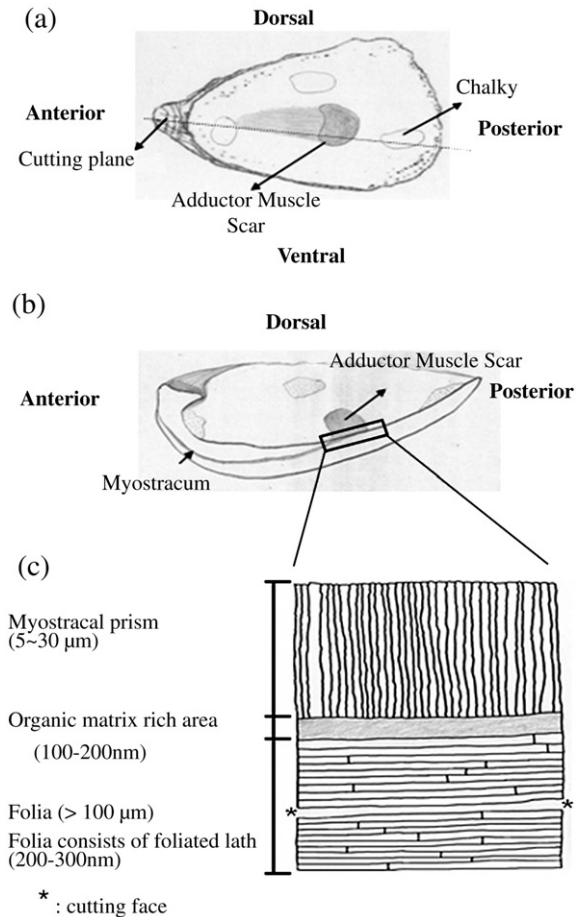
Fig. 1. Schematic illustration showing the structure of oyster shell [adapted from Lee and Choi, 2007]. (a) Schematic of inner surface of left valve (*Crassostrea gigas*). (b) Schematic of cross-sectional surface of cutting adductor muscle scar. (c) An enlargement indicating thickness dimensions of the myostracal prism, organic rich area, and folia. The size of each layer is exaggerated for clarity. Various terms are in common use in description of the bivalve shell (Galtsoff 1964; Cariker and Palmer 1979a; Waller 1971). The samples including myostracum and folia under adductor muscle scar are only used in this study.

Lausanne, Swiss) for confirmation were used. Parameters used in simulation are as follows:

Lattice	Rhombohedral
Space group	R-3c (167)
Cell parameter	$a=4.9896$ ang, $c=17.0610$ ang (hexagonal cell)
Atomic coordinates	Ca (6b) $x=0$, $y=0$, $z=0$
	C (6a) $x=0$, $y=0$, $z=0.25$
	O (6e) $x=0.257$, $y=0$, $z=0.25$
JCPDS	47–1743
Cleavage	(10–14)

2.3. Micro/Nanoindentation

Nanoindentation tests were performed using a Nanoindenter XP Testing System (MTS) in conjunction with the CSM (Continuous Stiffness Measurements). The Hysitron nanoindenter monitors and records the dynamic load and displacement of the indenter, a diamond Berkovich three-sided

(a)

(b)
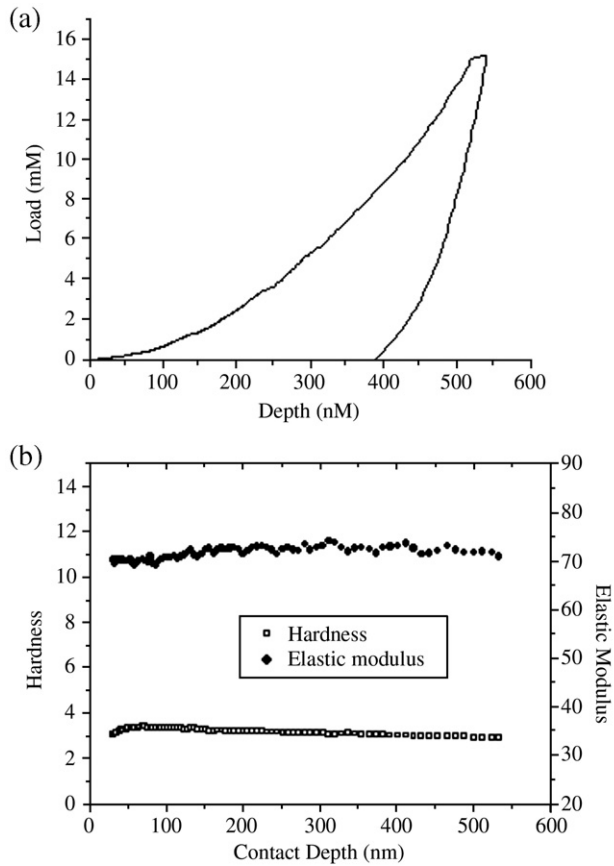
Fig. 2. Results from mechanical testing and analysis performed on polished shell samples. Hardness and elastic modulus values are obtained from nanoindentations perpendicular to the cross-sectional surface. The measured hardness of the folia was 3.2 ± 0.1 GPa and the elastic modulus was 73 ± 1.2 GPa.

pyramid, with a force resolution of 50 nN and displacement resolution of 0.1 nm. Hardness and elastic modulus properties were calculated from the recorded load–displacement curves. A microhardness tester with a diamond Vickers four-sided pyramid indenter was used to measure the microhardness values in the polished shell samples. Indentations were made with a normal load of 2 N held for 10 s. The indentation impressions and associated crack were examined using the environmental SEM (FEI XL-30 FE-SEM).

3. Results

In the oyster shell, the folia serve as a template in the same way that a human skeleton does [9]; they therefore need to have favorable mechanical properties such as tensile strength and elastic modulus. Considering the amounts of the organic matrix in the boundary surface and the value of the elastic modulus of the folia, the folia in the oyster shell of *C. gigas* have unique characteristics to enable any external impact to be minimized, ensuring the survival of the living tissues inside. The characteristic structures of the adult shell of the oyster, *C. gigas*, are as follows: an interior view of the left valve (Fig. 1a), cut surface of adductor muscle scar (Fig. 1b) and the schematic of biomineral structure and organic-rich area at

the interface between the myostracum and folia (Fig. 1c). The myostracal prisms are 5–30 μm in length, running from the umbo direction to the adductor muscle (Fig. 1b), with a prismatic form. On the other hand, the folia are more than 100 μm thick, with each single layer being 200–300 nm in size (Fig. 1c). Each lath is typically about 1–3 μm wide and about 200–300 nm thick.

(a)

(b)
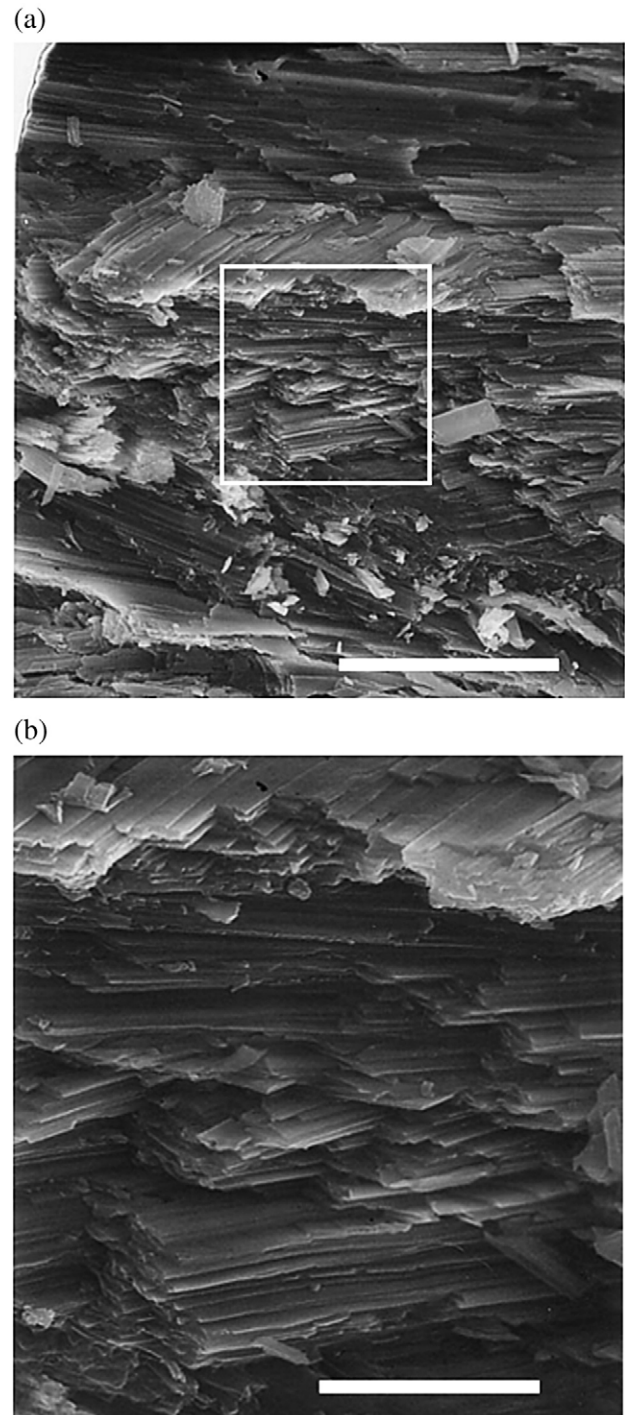
Fig. 3. SEM of (a) fractured folia under myostracum and (b) an enlargement of the inset in (a). The fractured folia seem to be the extreme disorganization of laths but the enlargement image shows the laths to consist of clusters that have the same orientation. Scale bars are 30 μm and 10 μm, respectively.
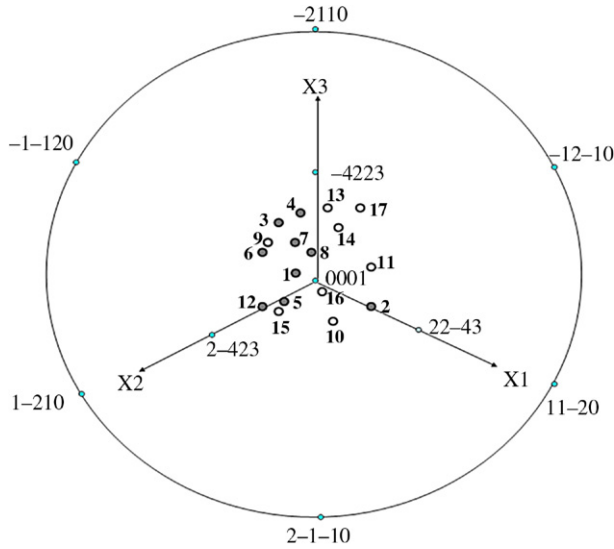
Fig. 4. Stereographic projection of (0001) plane of folia. The number of tiles analyzed by the Kikuchi pattern is seventeen (full circle: $w>0$, open circle: $w<0$).

Multiple partial loading/unloading nanoindentations made on polished folia samples were used to determine the hardness and elastic modulus as a function of depth. The results are shown in Fig. 2, along with hardness and elastic modulus values that were calculated from the load–displacement curve using standard techniques [10]. A typical load–displacement curve, as shown in Fig. 2a, indicates plastic deformation of the folia. The hardness was determined to be 3.2 ± 0.1 GPa, and the elastic modulus was found to be 73 ± 1.2 GPa (Fig. 2b). Wang et al. [11] reported that the microhardness of the sea urchin teeth composed of calcitic fibers ranges from a low value of 140 kg mm^{-2} to a high value of 360 kg mm^{-2}. They explain that the reason for the higher values of microhardness in urchin teeth is due to magnesium occlusion. The occlusion of magnesium into the calcite crystal lattice causes lattice distortion, which in turn increases the sliding resistance of dislocations and the deformation resistance of the crystals. Compared with urchin teeth consisting only of calcite, these urchin teeth show a high level of microhardness but with a large variation in hardness

Table 1
Summary of zone axis orientation and calculated angle of foliated laths

No.	Zone axis			Angle [a] (°)	No.	Zone axis			Angle [a] (°)
	u	v	w			u	v	w	
1	−223	−439	2646	0	10	1050	−120	−2103	138.9
2	630	591	1515	110.3	11	41	1022	−1845	151.7
3	−879	48	2337	34.8	12	924	−1119	2595	53.5
4	−948	201	2415	40.2	13	−1288	1325	−2361	116.0
5	929	−948	2688	56.6	14	−1067	1252	−2481	122.7
6	−239	−740	2136	18.0	15	912	−918	−2706	110.6
7	−602	−104	2574	22.7	16	411	−111	−2907	147.1
8	−623	565	2877	57.2	17	−935	1306	−2424	127.8
9	−353	−497	−2397	88.5					

[a] The calculated angle between zone axis of each lath and that of No. 1 (−223 −439 2646).

(220 kg mm^{-2}) that changes depending upon the region and the magnesium concentration.

The SEM (scanning electron microscopy) image in Fig. 3 shows the cross-section of fractured folia under the myostracum. As shown in Fig. 3b, foliated laths, which constitute folia, exist in the form of clusters having the same orientation.

Using the Kikuchi patterns obtained by TEM (transmission electron microscopy), the orientation of each of 17 foliated laths

(a)

(b)
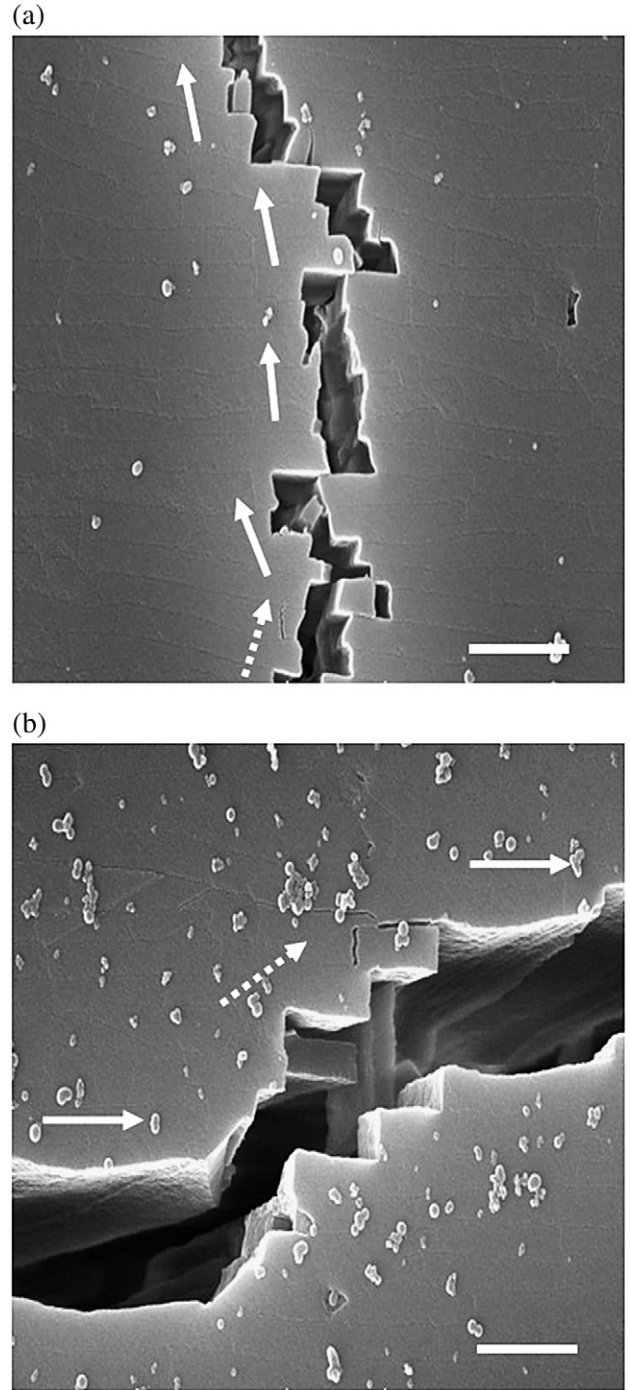
Fig. 5. Crack morphologies of folia on the cross-sectional surface. The arrows in the figures show a direction of crack propagation: (a) SEM of the perpendicular area of the microindentation zone and (b) SEM of the parallel area of the microindentation zone. Scale bar is 1 μm.

constituting folia was analyzed (Fig. 4, Table 1). The stereographic pattern (001) shows the distribution of the zone axis of each lath arranged centering on the plane. From the picture (001), we can see that the distribution is made in a circular form centering on the plane (001), and plane and laths each have their own peculiar angle of planes. In order to evaluate the tilt of each lath, we set the exterior lath among the 17 foliate laths as the reference plane (No. 1 in Table 1) and then calculated the orientation of each lath (Table 1). As shown in Table 1, we found that the orientation of each lath is not the same, but is similar to one of two types. These two groups were divided into type I, which forms orientation within 90°, and type II, within >100° (see Table 1).

The path of the cracks of the folia propagating in the vertical and horizontal direction with respect to folia is shown in Fig. 5a and b, respectively. The vertical directional crack path, several foliated laths formed a group exhibiting the identical pattern of straight, vertical crack propagation. Each group was separated by short horizontal crack along the interface of folia. Exception to this behavior (dotted line with arrow) was also found. The crack formed along the horizontal direction also showed a regular and hierarchical crack pattern (Fig. 5b). Obviously, the mechanical properties (toughness, strength, etc) of the laminated structure in this part are optimal when the main crack propagates perpendicular to the interface plane. They are much weaker when the main crack propagates parallel to the interface.

4. Discussion

Folia occupy 60–70% by volume of the shell. It is interesting to note that the construction of the oyster shell is quite different from the nacre layer in abalone (Fig. 1). When compared with nacre, it can be seen that it has the same laminated layer as nacre on the morphology in the direction of the c axis. However, oyster shell folia consist of calcite (rhombohedral), while nacre consists of aragonite (orthorhombic) [12].

Hardness and elastic modulus are important mechanical properties of all shells, which need to be optimized to protect the living body inside. The folia purely consisting of calcium carbonate have a constant hardness regardless of the region (Fig. 2b). It has also been shown that the hardness of folia is similar to the maximum hardness of urchin teeth (3.2 GPa corresponds to 325 kg mm^{-2} by unit conversion) [11]. This result shows that the density of organic and inorganic components in the folia is uniform. It has been reported that the elastic modulus of nacre consisting of aragonite is 50 GPa [13], but Li and Nardi [14] have stated that the elastic modulus of scallop shell, which consists of multilayers of aragonite and has a crossed lamellar structure in which each layer has different orientation, is 87 GPa. Menig et al. [15] reported that the strength and toughness of conch shell, which has "plywood" structure characteristics and consists of aragonite, are much higher than those of calcium carbonate, which is described as mineral. They also reported that conch shell has outstanding mechanical properties due to the effects of the organic layers distributed on the boundary of each layer and the preferred orientations of the multilayered structure. Of course,

there is some uncertainty about a given shell's history, including its age and degree of hydration. As such, we know that the comparison of the mechanical properties of these shells requires a statistical analysis in order to be quantitatively evaluated. However, when considering that folia consist of calcite and differ in their organic matrix from scallop shell and conch shell, which belong to nacre, it can be assumed that the orientation of the folia can also affect the material properties of the adult shell of *C. gigas*. In addition, from the results above, we can see that folia consisting of calcite have much better mechanical properties than any other biomineral components consisting of calcitic layers. In light of these considerations it is very appropriate that the majority of the shell's volume is built of the folia.

A foliated structure does not fracture as cleanly at the intercrystalline organic matrices as a prismatic structure does [9], but fractures do provide valuable information about the form of laths.

The statistical chart of direction in Table 1 and Fig. 4 reveals that type I and type II have about the same proportion and are concentrated within a range of 60° (from 18° to 88°) or 41° (from 110° to 151°), respectively (Table 1). We observed that both type I and type II consist of some clusters (Table 1: Nos. 3–8, Nos. 13–17). This result may lead to the inference that the orientation of tablets has some sort of regularity. Moreover, this result is consistent with the SEM image of fractured folia (Fig. 3).

Crack deflection is the most commonly observed phenomenon in nacre, especially when cracking occurs in a direction perpendicular to the aragonite layer [16]. Cracking occurs mainly along the direction normal to the aragonite layer, while the interfaces along the layers maintain close contact. Therefore, the binding forces between the organic phase and the aragonite layer will inhibit further development of the crack [17]. It has been reported that nacre grows in a "Christmas tree" pattern [18,19] and all tablets consisting of nacre along the same "Christmas tree" have the same crystallographic orientation [20]. Thus, it could be estimated that in the folia showing the same morphology as the laminated layer and having smaller quantity of the organic matrix than nacre, the pattern of crystal growth and morphology *in vivo* of the folia is different from that of nacre.

Obviously, the anisotropy of foliated lath is closely related to the highly ordered microarchitectural characteristics and would be the main reason for the mechanical properties of oyster shell.

The adult shell of *C. gigas* mostly consists of calcite and has lower hardness and relatively lower content of organic materials than aragonite has. As one of the means to make up for this shortcoming, we can assume that the orientations of folia in *C. gigas* are adjusted. Normal calcite would show a brittle cleavage parallel to the {10–14} crystallographic lattice planes that define the typical calcite rhombohedra [21]. This modification of the material properties has already been reported for biogenic calcite [22,23]. However, most of the reports about biogenic calcite have dealt only with the calcareous spicule of the sea urchin, which seems to have a conchoidal fracture pattern. From the result of the crack test of folia, we can see that folia in the oyster shell also have an anisotropic fracture pattern, which was previously observed in the lamellar structure (Fig. 5).

5. Conclusions

From this study, we could firstly see that the folia in the oyster shell of *Crassostrea gigas* have a peculiar orientation which is distinguished from any other biomineral consisting of calcite, as well as nacre which has the same lamellar structure. The fracture and microindentation zone morphologies, as well as cracking behavior of the folia, are anisotropic, and strongly reflect its microstructural character. Regular and periodic fracture pattern of folia is due to the interaction between cleavage plane (104) and grouped type I and type II orientations of folia. This will be a result of the high order of hierarchy in this nanostructure, which leads to crack deflection and arrest at inter-lamellar boundaries, enhancing the material's resistance to fracture. Comparing the mechanical properties and the amount of organic matrix of folia with those of nacre, these structural features of folia may have a relationship with the survival strategy of *C. gigas* through the two different orientation types in order to make up for relatively lower hardness and lower quantity of organic matrix which is due to the fact that the adult oyster shell mostly consists of calcite. It is recommended that an in-depth study on this topic should be conducted in the near future.

References

[1] M. Sarikaya, Proc. Natl. Acad. Sci. U. S. A. 96 (1999) 14183.
[2] G. Mayer, M. Sarikaya, Exp. Mech. 42 (2002) 395.
[3] I.A. Aksay, S. Weiner, Curr. Opin. Solid State Mater. Sci. 3 (1998) 219.
[4] D.L. Kaplan, Curr. Opin. Solid State Mater. Sci. 3 (1998) 232.
[5] H. Tong, J.M. Hu, W.T. Ma, G.R. Zhong, S.N. Yao, N.X. Cao, Biomaterials 23 (2002) 2593.
[6] H.B. Stenzel, Science 145 (1964) 155.
[7] K.J. Westin, A.C. Rasmuson, J. Colloid Interface Sci. 282 (2005) 359.
[8] C.S. Sikes, A.P. Wheeler, A. Wierzbicki, A.S. Mount, R.M. Dillaman, Biol. Bull. 198 (2000) 50.
[9] M.R. Carriker, in: V.S. Kennedy, I.E. Newell Roger, A.E. Eble (Eds.), The Eastern Oyster *Crassostrea virginica*, Mayland Sea Grant College, 1996, p. 75.
[10] X. Li, B. Bhushan, Mater. Charact. 48 (2002) 11.
[11] R.Z. Wang, L. Addadi, S. Weiner, Philos. Trans. R. Soc. Lond., B 352 (1997) 469.
[12] H.D. Megaw, Crystal Structures: a Working Approach, West Washington Square, Philadelphia, PA, 1973.
[13] D.R. Katti, K.S. Katti, Mater. Res. Soc. Symp. Proc. 599 (2000) 231.
[14] X. Li, P. Nardi, Nanotechnology 15 (2004) 211.
[15] R. Menig, M.H. Meyers, M.A. Meyers, K.S. Vecchio, Mater. Sci. Eng., A Struct. Mater.: Prop. Microstruct. Process. 297 (2001) 203.
[16] R.Z. Wang, H.B. Wen, F.Z. Cui, H.B. Zhang, H.D. Li, J. Mater. Sci. 30 (1995) 2299.
[17] Q.L. Feng, F.Z. Cui, G. Pu, R.Z. Wang, H.D. Li, Mater. Sci. Eng., C, Biomim. Mater., Sens. Syst. 11 (2000) 19.
[18] S. Shen, A.M. Belcher, P.K. Hansma, G.D.S. Stucky, D.E. Morse, J. Biol. Chem. 272 (1997) 32472.
[19] M. Fritz, D.E. Morse, Col. Int. Sci. 3 (1998) 55.
[20] A. Lin, M.A. Meyers, Mater. Sci. Eng., A Struct. Mater.: Prop. Microstruct. Process. 390 (2005) 27.
[21] I. Sethmann, R. Hinrichs, G. Worheide, A. Putnis, J. Inorg. Biochem. 100 (2006) 88.
[22] J. Aizenberg, J. Hanson, M. Ilan, L. Leiserowitz, T.F. Koetzle, L. Addadi, S. Weiner, FASEB J. 9 (1995) 262.
[23] Y. Politi, T. Arad, E. Klein, S. Weiner, L. Addadi, Sicence 306 (2004) 1161.